

## PARAMETRIC VIBRATIONS OF PIPES INDUCED BY PULSATING FLOWS IN HYDRAULIC SYSTEMS

JAN ŁUCZKO, ANDRZEJ CZERWIŃSKI

*Cracow University of Technology, Faculty of Mechanical Engineering, Kraków, Poland*

*e-mail: jluczko@mech.pk.edu.pl; ac@mech.pk.edu.pl*

The paper discusses the model of transverse vibrations of a pipe induced by flow velocity pulsation. The motion is described by a system of two non-linear partial differential equations with periodically variable coefficients. The analysis uses the Galerkin method with orthogonal polynomials as the shape functions. The instability regions are determined by Floquet's method. The influence of selected parameters on natural frequencies and on the character and level of vibrations is studied. The possibility of the excitation of periodic and quasi-periodic oscillations is demonstrated. The results of theoretical analysis are compared with the experimental data.

*Keywords:* hydraulic systems, flow-induced vibration, parametric resonance

### 1. Introduction

Vibrations in hydraulic systems may be induced by fluid flows as well as mechanical sources of vibration. Components of hydraulic systems such as pumps, hydraulic engines and valves generate pulsation of fluid flow. On the other hand, vibrations in the system can be induced by unbalanced and misaligned rotating parts of the drive system as well as time variable forces and moments acting upon the hydraulic system components.

Vibrations of hydraulic pipes can be caused by factors associated with fluid flow or due to mechanical excitations. Vibrating elements such as hydraulic pumps as well as vibration of the supporting structure can become the source of kinematic excitations. Vibration propagation is facilitated by a rigid connection between the frame, system components and interconnecting pipes and hoses.

Furthermore, hydraulic lines are subjected to loads and vibrations caused by fluid flow. These include pulse loads resulting from valve operation (e.g. water hammer effect) as well as time varying forces resulting from pressure pulsation.

As regards certain critical flow parameters (velocity, pressure) in a particular line, the conditions can arise leading to the loss of stability (Holmes, 1978). The critical values depend mainly on the structure and geometry of the pipe or hose. In turn, the parametric resonance phenomenon occurs when the fluid flow velocity changes periodically (Gregory and Paidoussis, 1966a,b). The phenomenon can occur at a specific amplitude and frequency of pulsation flow and at a sufficiently high flow velocity.

The pipe model with a pulsating fluid flow was first investigated by Ginsberg (1973) for pinned-pinned pipes, then by Paidoussis and Issid (1974) for cantilevered pipes and by Paidoussis and Sundararajan (1975) for clamped-clamped pipes. The calculation results were then verified by the authors of the experiment (Paidoussis and Issid, 1976).

In their work, Semler and Paidoussis (1994) compared the underlying assumptions and derivation procedures employed by authors of several publications on the subject of non-linear dynamic behaviour of cantilevered and clamped-clamped pipes. They also discussed the adequacy of equations derived by different authors and proposed the most complete equation for

the clamped-clamped pipe. The comprehensive survey of modelling methods is given in the monograph (Paidoussis, 1998).

Dynamic behaviour of continuous systems, such as beams, moving tapes or pipes with the flowing fluid is governed by non-linear partial differential equations with appropriate boundary and initial conditions. In general, the exact solutions are impossible and hence approximate methods need to be developed. Thus obtained results have to be verified experimentally.

This paper focuses on the development of effective methods for testing the impact of system parameters on the range of the instability areas and elevated levels of vibration. In the available literature, there are few results of such research. Typically, the dynamic analysis is carried out for fixed values of the system (Gorman *et al.*, 2000; Lee and Chung, 2002; Panda and Kar, 2008), alternatively, bifurcation diagrams are obtained, showing the influence of the selected parameter (one-parameter diagrams) on the type of thus induced vibrations (Wang, 2009). Few works only summarize the results of testing how two concurrent parameters should affect the stability of linear systems. For example, Kadoli and Canesan (2004) tested the effect of temperature on the regions of stability in the plane determined by the flow velocity and flow pulsation frequency using the Floquet method.

In this paper, the effectiveness of the proposed methods was verified by numerical calculations carried out for the hose model. Predicted results were compared with experimental data.

## 2. The model of the system

Equations of motion of a hose conveying fluid and fixed on both ends are based on the following assumptions: the hose diameter is small compared with its length, which allows the Euler-Bernoulli beam model to be used, the shape and dimensions of the hose cross-section remain unchanged, the hose motion takes place in the plane, the fluid is incompressible, the fluid velocity is constant in the hose cross-section and does not change along its length.

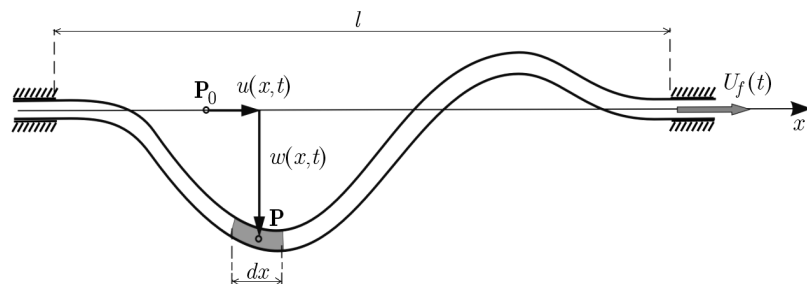


Fig. 1. Model of the system

The model of the investigated system is shown in Fig. 1. For the description of transverse and longitudinal vibrations of the hose of length  $l$ , the coordinates  $w(x, t)$  and  $u(x, t)$  are introduced. The relative motion of the fluid is determined by the velocity  $U_f(t)$ . Differential equations of motion can be derived from the law of momentum. For this purpose, the fluid element and the hose element are analysed separately.

The fluid element with a unit mass  $m_f$  is subjected to applied pressure forces  $pA$  (where:  $p$  – pressure,  $A$  – cross-section area) and normal and tangential components of internal forces acting in the fluid-hose system. Apart from the internal forces, the hose element of a unit mass  $m_p$  is subjected to the action of transverse forces  $Q$ , axial forces  $T$  and bending moments  $M$ . Adding the respective sides of the equations of motion of the fluid and the hose, gives equations independent on the internal forces

$$\begin{aligned}
 m_f \left( \frac{D^2 u}{Dt^2} + \frac{\partial U_f}{\partial t} \right) + m_p \frac{\partial^2 u}{\partial t^2} + \frac{\partial}{\partial x} [(pA - T) \cos \varphi] + \frac{\partial}{\partial x} (Q \sin \varphi) &= 0 \\
 m_f \frac{D^2 w}{Dt^2} + m_p \frac{\partial^2 w}{\partial t^2} + \frac{\partial}{\partial x} [(pA - T) \sin \varphi] - \frac{\partial}{\partial x} (Q \cos \varphi) - (m_p + m_f)g &= 0
 \end{aligned}
 \tag{2.1}$$

where the absolute derivatives present in Eqs. (2.1) are derived from the following formulas

$$\frac{D^2 v}{Dt^2} = \frac{\partial^2 v}{\partial t^2} + U_f^2 \frac{\partial^2 v}{\partial x^2} + 2U_f \frac{\partial^2 v}{\partial x \partial t} + \frac{\partial U_f}{\partial t} \frac{\partial v}{\partial x}
 \tag{2.2}$$

where  $v(x, t) = u(x, t)$  or  $v(x, t) = w(x, t)$ . The angle  $\varphi$ , indicating the direction of the tangent to the pipe axis depends on the coordinates  $u$  and  $w$ .

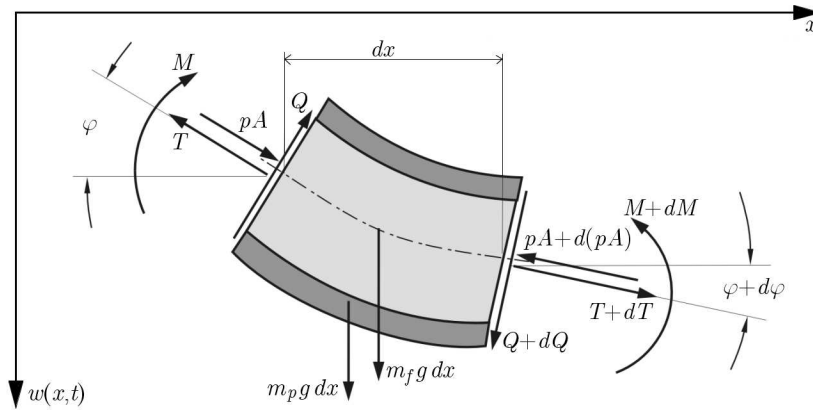


Fig. 2. Fluid and pipe elements

For brevity, differentiation with respect to the variable  $t$  is marked by a dot and differentiation with respect to the variable  $x$  is indicated by a prime symbol. To determine the value of the axial force  $T$  and the bending moment  $M$ , the influence of internal damping is taken into account, basing on the Voigt-Kelvin hypothesis

$$T = T_s + EA_p(\varepsilon + \alpha \dot{\varepsilon}) \quad M = -EI_p(\varphi' + \alpha \dot{\varphi}')
 \tag{2.3}$$

where  $T_s$  is the static component and  $\alpha$  is the damping coefficient. The transverse force  $Q$  is derived from the relevant equation by taking into account the axial strain  $\varepsilon$  of neutral line

$$Q = (1 + \varepsilon)^{-1} M'
 \tag{2.4}$$

where the axial strain  $\varepsilon$  can be determined from the dependence

$$\varepsilon = \sqrt{(1 + u')^2 + w'^2} - 1
 \tag{2.5}$$

Equations (2.1)-(2.5) are the starting point for deriving approximate equations that describe hose vibration induced by the flow. They can sometimes be reduced to two non-linear partial differential equations. Taking into account the approximate formula proposed by Paidoussis (1998), we get

$$(pA - T)' = -m_f \dot{U}_f
 \tag{2.6}$$

These equations are not dependent on the flow resistance. Assuming that the axial displacements are an order smaller than the transverse displacements  $w \sim O(\epsilon)$ ,  $u \sim O(\epsilon^2)$ ,  $\epsilon \ll 1$ , then when

non-linear terms in the Taylor series are expanded, the equations describing the vibrations of the hose with an accuracy of  $O(\epsilon^3)$  become

$$\begin{aligned}
& m\ddot{u} - EA_p(u'' + \alpha\dot{u}'') + m_f\left(\dot{U}_f u' + 2U_f \dot{u}' + U_f^2 u'' + \frac{1}{2}\dot{U}_f w'^2\right) \\
& - [p_0 A(1 - 2\nu) - T_0 + m_f \dot{U}_f(l - x)]w'w'' - EA_p[w'w'' + \alpha(w''\dot{w}' + w'\dot{w}'')] \\
& - EI_p[(w''''w' + w''''w'') + \alpha(\dot{w}''''w' + \dot{w}''''w'')] = 0 \\
& m\ddot{w} + m_f\left[2U_f \dot{w}' + U_f^2 w'' + \dot{U}_f\left(u'w' + \frac{1}{2}w'^3\right)\right] + EI_p(w'''' + \alpha\dot{w}''''') - mg \\
& + [p_0 A(1 - 2\nu) - T_0 + m_f \dot{U}_f(l - x)]\left(w'' - w'u'' - w''u' - \frac{3}{2}w'^2 w''\right) \\
& + EA_p\left(u''w' + u'w'' + \frac{3}{2}w'^2 w''\right) + \alpha EA_p(\dot{u}''w' + \dot{u}'w'' + w'^2 \dot{w}'' + 2w'\dot{w}''w'') \\
& - EI_p(2w''''u' + 4w''''u'' + 3w''''u''' + w'u'''' + 2w''''w'^2 + 8w'u''w'' + 2w''''^3) \\
& - \alpha EI_p(2\dot{w}''''w'^2 + 2\dot{w}''''w'u' + 6w''''\dot{w}''w' + 6w''''\dot{w}'w'' + 8\dot{w}''''w''w' + 6\dot{w}''''w''^2 \\
& + 2\dot{w}''''u' + 4\dot{w}''''u'' + 3\dot{w}''''u''' + \dot{w}'u'''' + w''''\dot{u}' + 3w''''\dot{u}'' + 3w''''\dot{u}''' + w'\dot{u}''''') = 0
\end{aligned} \tag{2.7}$$

In particular, for  $U_f = \text{const}$  and  $\alpha = 0$ , Eqs. (2.7) are identical to those proposed by Paidoussis (2003). Equations (2.7) contain variable coefficients on account of the dependence of the flow velocity  $U_f$  on time. The velocity change was assumed to be harmonic

$$U_f = U_{f0}[1 + A_U \sin(\omega t)] \tag{2.8}$$

where  $U_{f0}$  and  $\omega$  are the mean velocity and frequency and  $A_U$  is the dimensionless amplitude of pulsation.

### 3. The method of analysis

Non-linear partial differential equations (2.7) are solved by the Galerkin method (Czerwiński and Łuczko, 2012; Lee and Chung, 2002; Łuczko and Czerwiński, 2012; Udar and Datta, 2007), assuming an approximate solution

$$w(x, t) = \sum_{j=1}^N \varphi_j(x)z_j(t) \quad u(x, t) = \sum_{j=1}^N \psi_j(x)y_j(t) \tag{3.1}$$

The shape functions  $\varphi_j(x)$  and  $\psi_j(x)$  must satisfy the boundary conditions and should create a complete set of functions. In the case of simply supported pipes, the trigonometric functions can be used, yet when the analysis of non-linear problems involves different boundary conditions, polynomial functions may prove more appropriate. To construct the approximating polynomial function, a system of linearly independent functions  $\phi_1(x), \phi_2(x), \dots, \phi_N(x)$  is developed, satisfying certain boundary conditions in the interval  $(0, l)$ . A polynomial form of these functions is assumed

$$\phi_j(x) = a_{0j} + a_{1j}x + a_{2j}x^2 + \dots + a_{j+3,j}x^{j+3} = \sum_{k=0}^{j+3} a_{kj}x^k \quad j = 1, 2, \dots, N \tag{3.2}$$

Functions describing the transverse displacement must satisfy four boundary conditions. These boundary conditions being applied, for any parameters  $a_{4j}, a_{5j}, \dots, a_{nj}$ , where  $n = j + 3$  the first four coefficients  $a_{0j}, a_{1j}, a_{2j}, a_{3j}$  of solutions (3.2) can be determined. For a fixed-fixed hose, the following boundary conditions have to be satisfied

$$\phi_j(0) = \phi_j'(0) = \phi_j(l) = \phi_j'(l) = 0 \tag{3.3}$$

Conditions for  $x = 0$  finally yield  $a_{0j} = a_{1j} = 0$ . For other boundary conditions (for  $x = l$ ), we get the equation

$$a_{2j} + a_{3j} = - \sum_{k=4}^{j+3} a_{kj} \quad 2a_{2j} + 3a_{3j} = - \sum_{k=4}^{j+3} ka_{kj} \quad (3.4)$$

determining the coefficients  $a_{2j}$  and  $a_{3j}$  in the polynomial of the degree  $j + 3$ . It can be assumed:  $a_{kj} = 1$  for  $4 \leq k \leq j + 3$  ( $j = 1, 2, \dots, N$ ). Thus the obtained polynomials are not orthogonal. The base of orthonormal polynomials  $\varphi_1(x), \varphi_2(x), \dots, \varphi_N(x)$  is typically obtained by the Gram-Schmidt orthogonalization method. The subsequent polynomials are defined by the recurrent formula

$$\varphi_j(x) = \frac{\vartheta_j(x)}{\sqrt{\int_0^1 \vartheta_j^2(\xi) d\xi}} \quad (3.5)$$

where

$$\vartheta_j(x) = \phi_j(x) - \sum_{k=1}^{j-1} \varphi_k(x) \sqrt{\int_0^l \phi_j(\xi) \varphi_k(\xi) d\xi} \quad (3.6)$$

and  $\vartheta_1(x) = \phi_1(x)$ . In the case of a linear model, the transverse vibration equation is not dependent on the variable  $u$ . Therefore, the linear analysis can be carried out by investigating the equation of transverse vibrations only. With the Galerkin method being applied and the vector  $\mathbf{z} = [z_1, z_2, \dots, z_N]^T$  introduced, the system of ordinary differential equations can be rewritten in a concise matrix form

$$\ddot{\mathbf{z}} + \mathbf{B}\dot{\mathbf{z}} + \mathbf{C}\mathbf{z} = \mathbf{0} \quad (3.7)$$

where  $\mathbf{C}$  is the stiffness matrix and  $\mathbf{B}$  takes into account the damping and gyroscopic effects. When the numerical methods are applied in stability analysis, the solution to Eq. (3.7) is expressed as

$$\dot{\mathbf{v}} = \mathbf{A}\mathbf{v} \quad (3.8)$$

where

$$\mathbf{v} = \begin{bmatrix} \mathbf{z} \\ \dot{\mathbf{z}} \end{bmatrix} \quad \mathbf{A} = \begin{bmatrix} \mathbf{0} & \mathbf{I} \\ -\mathbf{C} & -\mathbf{B} \end{bmatrix} \quad (3.9)$$

Using numerical procedures, the eigenvalues of the matrix  $\mathbf{A}$  can be derived accordingly. The imaginary parts of the eigenvalues define the natural frequencies whilst the sign of the real parts gives information as to the stability of solutions.

Since Eq. (3.8) is a linear equation with periodically variable coefficients (period  $T = 2\pi/\omega$ ) the stability regions can be determined by Floquet's method. For that purpose, the monodromy matrix is derived  $\mathbf{M} = \mathbf{F}(T)$ , defined by the fundamental matrix  $\mathbf{F}$ , satisfying the following differential matrix equation

$$\frac{d\mathbf{F}}{d\tau} = \mathbf{A}\mathbf{F} \quad (3.10)$$

and the boundary conditions

$$\mathbf{F}(0) = \mathbf{I} \quad (3.11)$$

The eigenvalues  $\mu_k$  of the monodromy matrix, referred to as characteristic multipliers of the system, determine the stability of periodic solutions. When at least one multiplier satisfies the inequality  $|\mu_k| > 1$ , the solution will be unstable. The characteristic multipliers are obtained by solving the following eigenvalue problem

$$(\mathbf{M} - \mu\mathbf{I})\mathbf{u} = \mathbf{0} \quad (3.12)$$

Analysing the condition  $|\mu_k| > 1$ , the instability regions can be determined in the space of selected system parameters.

#### 4. The results of numerical simulations and experiments

The numerical procedure was applied and experimental tests were performed on a model of an elastic hose fixed on both ends. The parameters considered in the study were: hose length  $l = 1.92$  m, outside diameter  $d_z = 0.021$  m, inside diameter  $d_w = 0.0127$  m, hose density  $\rho_p = 1870$  kg/m<sup>3</sup>, oil density  $\rho_f = 900$  kg/m<sup>3</sup>. The Young modulus obtained experimentally was equal to  $E = 20$  MPa, axial force  $T_0 = 80$  N and the damping coefficient  $\alpha = 0.05$  s. Throughout the experimental and numerical procedure, the average flow rate  $U_{f0}$  was varied in the range 0-8 m/s, the pressure at the end of the hose  $p_0$  varied in the range (0-10 MPa), the frequency of velocity pulsation  $f$  varied in the range (2-50 Hz) and the relative amplitude of pulsation  $A_U$  ranged from 0.15 to 0.25.

To find out how the natural frequencies and the instability ranges depend on those parameters, the linear model described by differential equation (3.7) with variable coefficients is investigated. The Galerkin method is employed and the first five modes of vibration are considered with the shape functions being assumed in form of orthogonal polynomials (3.5). The instability regions are determined by the numerical approach using Floquet's theory. The natural frequencies were determined assuming the fixed flow velocity and the stability tests were performed assuming that the flow velocity should vary in time in accordance with formula (2.8).

When testing the influence of parameters on the stability of solutions, it is required that the monodromy matrix elements should be determined by numerically integrating matrix equation (3.10) in a recursive procedure. To ensure the required accuracy level and to minimize the calculation time, it is recommended to use analytical formulas to determine the elements of the matrices  $\mathbf{B}$  and  $\mathbf{C}$ . These formulas are derived using the Maple 9 package. The program, written in Fortran, uses the procedures from the IMSL library to support numerical integration (Runge-Kutty-Verner's method of the 5th and 6th order and the Adams and Gear's method) and to solve the eigenvalue problems (QR algorithm applied to the matrix  $\mathbf{A}$  in the Hessenberg format).

To verify the numerical simulation results, an experimental setup was designed as shown in Fig. 3, allowing the control of the average flow velocity, pressure, amplitude and frequency of velocity pulsation. The liquid flow is generated by a multi-piston pump (II) driven by an electric motor (I). The variable capacity pump together with the accumulator (III) and the overflow valve (IV) are parts of the supply system with the stabilised, voltage-controlled pressure. The output from the supply system is connected to the input of the proportional directional control valve (Parker Df Plus). The valve enables most precise regulation of the flow rate in proportion to the applied input voltage. The fluid flows through the investigated hose (VII). Behind the hose, a throttling valve (VIII) is provided to stabilise the required pressure value.

The parameters associated with the flow (flow velocity, pressure) and the hydraulic hose dynamics are determined using the set of transducers. Flow velocity in the hose was computed basing on the flow rate readouts (from the flow rate meter  $Q$ ) and the hose cross-section area. Pressure measurements (pressure transducers  $p_1$  and  $p_2$ ) were taken at two points, directly

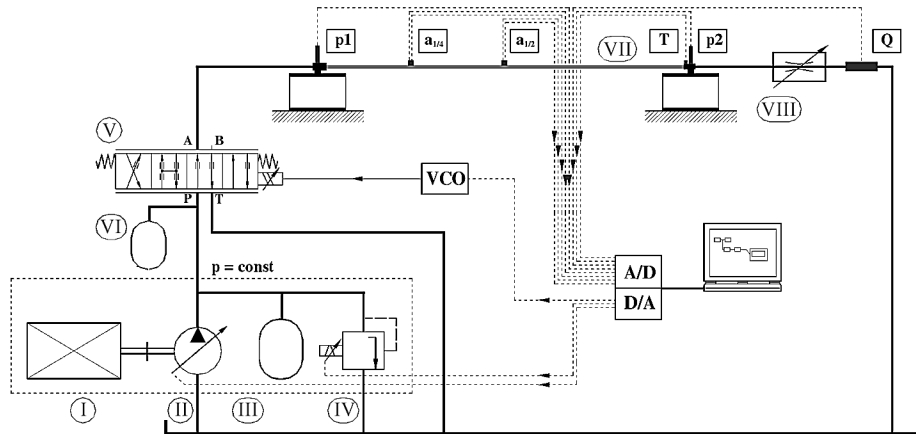


Fig. 3. Schematic of the experimental setup: I – electric motor, II – pump, III – hydropneumatic accumulator, IV – overflow valve, V – proportional directional control valve, VI – hydropneumatic accumulator, VII – investigated hose, VIII – throttling valve

upstream and downstream the hose section. The hose vibration parameters were measured with accelerometers ( $a_{1/2}$  and  $a_{1/4}$ ) located at the hose mid-length and at 1/4 of its length. Measurements of the hose temperature were taken with a contact sensor (a  $K$ -type thermocouple).

Signals from the transducers were fed to the computer via an  $A/D$  (NI USB-6009) card. Signal acquisition and processing was supported by the program DasyLab 11. Supported by the  $D/A$  card (NI USB-6009), the computer handled the settings of the pump and of the overflow valve and generated the control signal to the proportional directional control valve (using a voltage-regulated function generator).

In order that numerical and experimental data could be compared, the dimensional quantities were used even though the calculations were run on dimensionless ones. The first step was to establish the influence of flow velocity and pressure at the hose end on natural frequencies of the hose filled with the fluid flowing at a fixed rate. The results obtained in the analysis of linear model (3.8) are shown in Fig. 4.

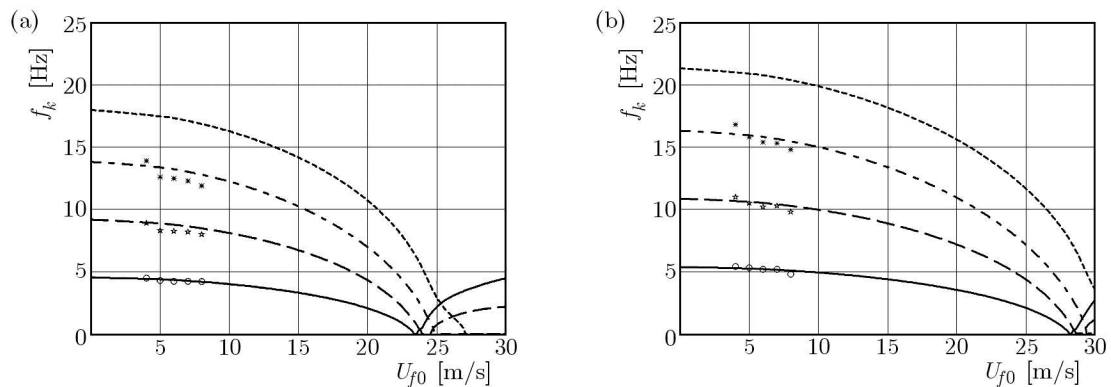


Fig. 4. The influence of flow velocity on natural frequencies: (a)  $p_0 = 2$  MPa, (b)  $p_0 = 4$  MPa

It appears that the parameters  $U_{f0}$  and  $p_0$  influence the natural frequencies of vibrations to a large extent. As the mean flow velocity increases, all frequencies tend to decrease whilst the fundamental frequency will be the first one to become zero. Decreasing frequency with increased flow velocity is the effect of the centrifugal inertia force (the term  $U_f^2 w''$  in Eq. (2.7)<sub>2</sub>, acting in opposite direction to the elasticity force. Flow velocity for which the natural frequency is zero is referred to as the critical velocity.

In the range of flow velocities higher than the critical velocity, the plots of frequency in Fig. 4 have interesting properties. The linear model is unstable in this range, yet when nonlinearities arising in this region are considered, some vibrations with limited amplitudes will become possible, too. The analysis of mode coefficients reveals that in the sub-critical range, subsequent frequencies correspond to particular modes of vibrations (3.5). In the post-critical range, a given mode is typically a combination of two or more modes.

Figure 4 gives the values of the first free natural frequencies obtained by running an experiment on a real object. In the laboratory conditions, the near-critical velocities could not be attained (the maximal velocity being about 10 m/s). Despite this limitation, it is reasonable to suppose that the values of characteristic parameters of the model were correct.

Results obtained for linear model (3.8) and for the non-linear one, governed by Eqs. (2.7), are compared in Fig. 5. Figure 5a illustrates the influence of flow velocity and flow pulsation frequency on the range of instability regions, determined according to Floquet's theory. Figure 5b demonstrates the influence of those parameters on the rms value of vibration velocity  $V_z$  in the direction transverse to the hose axis at the point distant from its attachment by 1/4 of its length. The graphs are plotted for  $p_0 = 2$  MPa and  $A_U = 0.2$ .

Figures 5a and 5b also plot the graphs of  $\omega = (\omega_n + \omega_m)/k$  ( $n, m = 1, 2, \dots, 5; k = 1, 2, \dots$ ) for selected values of  $n, m, k$  (the curves  $nm\_k$  expressing the dependence between the excitation frequency and combinations of natural frequencies). The form of the plots  $nm\_k$  depends on the average flow velocity  $U_{f0}$ . For the excitation frequency that satisfies the above relationships, the parametric resonance phenomenon should arise (Mailybayev and Seyranian, 2001; Udara and Datta, 2007). For example, for  $n = m = k = 1$  we get the fundamental resonance ( $\omega = 2\omega_1$  – plot 11\_1), and for  $n = k = 1, m = 2$  combination resonances will appear ( $\omega = \omega_1 + \omega_2$  – plot 12\_1).

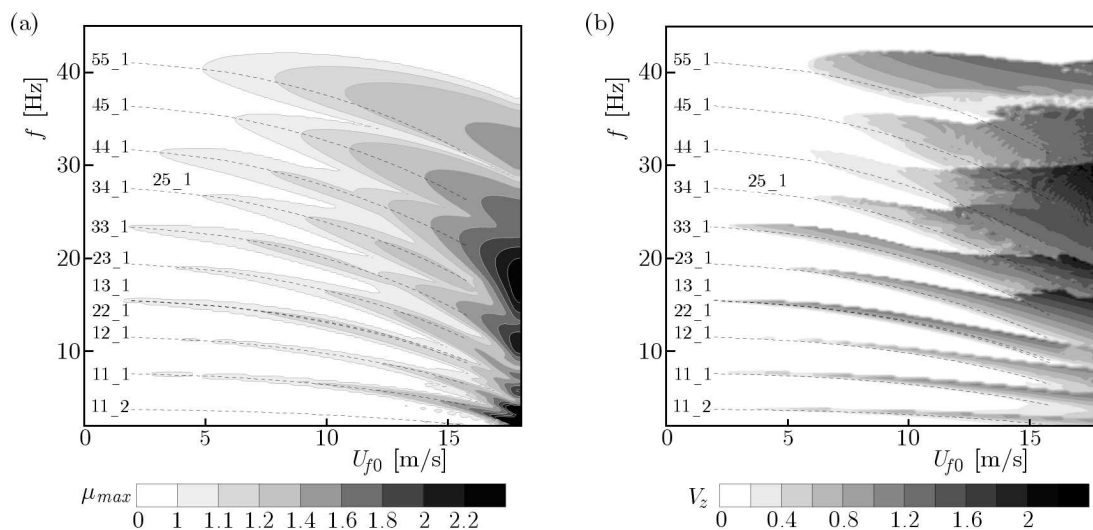


Fig. 5. The influence of flow velocity and flow pulsation frequency: (a) instability regions  $\mu_{max}$ , (b) rms value of vibration velocity  $V_z$  [m/s]

The distribution of the plane of parameters is sufficiently dense and uniform ( $200 \times 200$  points). The smoothness of curves limiting the instability regions (the plots of the maximal values of the characteristic multiplier  $\mu_{max}$  – Fig. 5a) and the zones of increased vibration level (Fig. 5b) prove the adequacy of the adopted approach. In the shaded areas (Fig. 5a) at least one of the characteristic multipliers is larger than one and hence in those areas the solutions to differential equation (3.8) will be unstable. Instability regions determined by Floquet's method envelop the curves  $nm\_k$  and expand with the increasing average flow velocity  $U_{f0}$ .

The linear analysis allows the stable regions to be promptly determined whilst the analysis of the non-linear model gives the properties of generated vibrations. In this case, the indicators can be derived that are associated with the amplitude of generated signals, and their dependence on the system parameters can be analysed accordingly. Furthermore, the character of the vibrations can be analysed as well as spectral analysis can be made in the case of periodic vibrations.

The plot in Fig. 5 is restricted to the sub-critical velocity range (the critical value  $U_{f0} \approx 24 \text{ m/s}$  – Fig. 4a), so the plotted results can be used only in the study of the parametric resonance phenomenon. The regions of increased vibration levels (Fig. 5b) agree well with the region of unstable solutions (Fig. 5b) based on the simplified model analysis.

Apart from the five regions of principal parametric resonance corresponding to the subsequent vibration modes (around the curves  $nm_k$ ), the investigated frequency range reveals the areas of combination resonance (in the proximity of plot curves 12\_1, 13\_1, 23\_1, 25\_1, 45\_1). The width of all these regions tends to increase with the flow pulsation frequency though the parametric resonance effect will occur in a higher frequency range provided that flow velocity is sufficiently large. The highest level of vibration intensity is registered for high flow velocities (the darkest areas in Fig. 5b). For velocities nearing the critical value, vibrations are excited regardless of the actual flow pulsation frequency but their character tends to change (these are often chaotic vibrations). However, as the critical values could not be attained in the experiments, no numerical results are provided.

To verify the model, the experimental results were compared with those predicted theoretically. In the course of experimental tests, the response of the system to excitations of variable frequency was obtained using the function generator *sweep*. The rms velocity values were established at two points distant from the attachment points by  $1/4$  and  $1/2$  of the hose length  $l$ . The parameters that were varied included the pressure  $p_0$  at the end of the hose, the average flow velocity  $U_{f0}$  and the dimensionless amplitude  $A_U$  (related to  $U_{f0}$ ) of pulsation. During the tests, the oil temperature was stabilised ( $55^\circ\text{C}$ – $65^\circ\text{C}$  on the average). Selected results are shown in Figs. 6a, 7a and 8a.

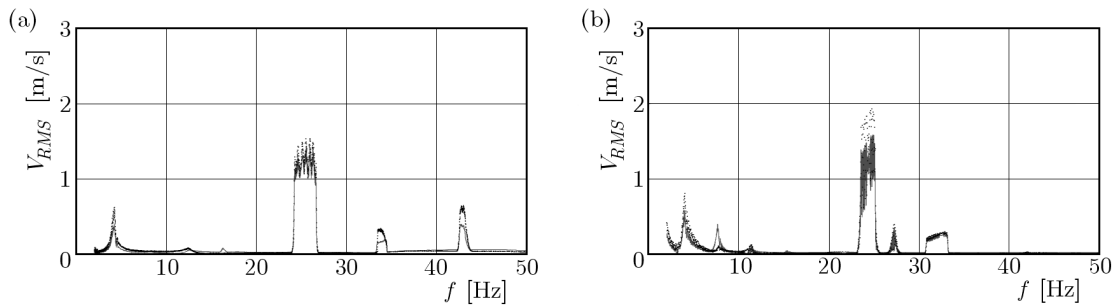


Fig. 6. The influence of flow pulsation frequency on the rms value of vibration velocity  $U_{f0} = 6 \text{ m/s}$ ,  $p_0 = 2 \text{ MPa}$ ,  $A_U = 0.2$ : (a) experimental results, (b) simulation results

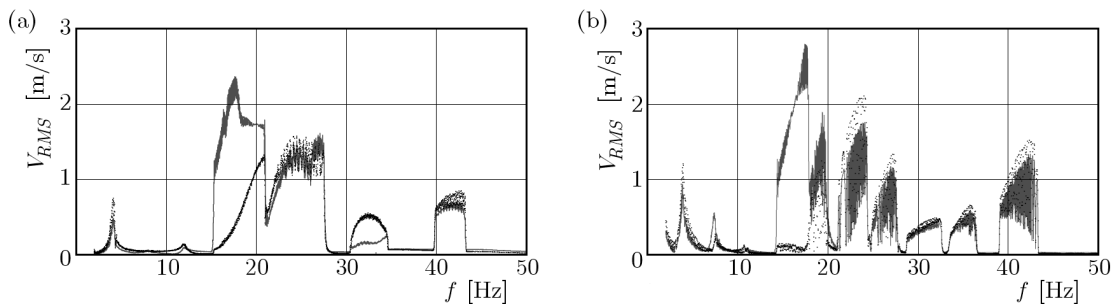


Fig. 7. The influence of flow pulsation frequency on the rms value of vibration velocity  $U_{f0} = 8 \text{ m/s}$ ,  $p_0 = 2 \text{ MPa}$ ,  $A_U = 0.2$ : (a) experimental results, (b) simulation results

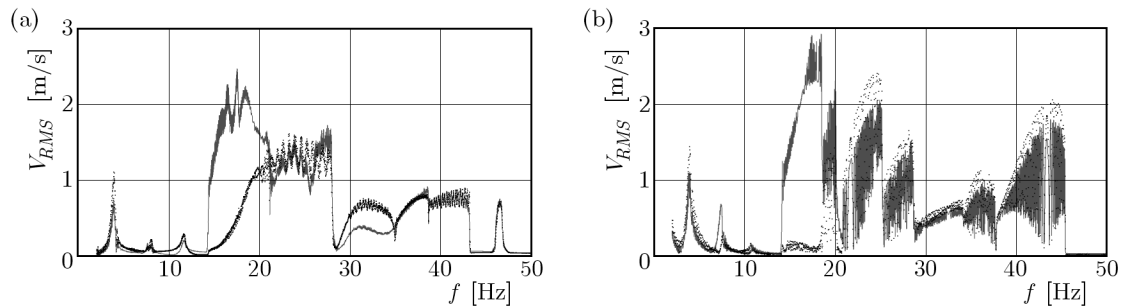


Fig. 8. The influence of flow pulsation frequency on the rms value of vibration velocity  $U_{f0} = 8$  m/s,  $p_0 = 2$  MPa,  $A_U = 0.25$ : (a) experimental results, (b) simulation results

The numerical procedure involved the modelling of the sweep generator, assuming the identical simulation time as in the experiments. The results corresponding to those summarized in Figs. 6a, 7a and 8a are shown in Figs. 6b, 7b and 8b. The continuous line applies to the measurement point  $x = l/4$ , the dotted line – to the point  $x = l/2$ .

Comparison of the results shows a good correspondence between the predicted and experimental results. Rms velocity values obtained by the numerical procedure and experimentally are similar, and so is similar the distribution of the relevant resonance ranges.

It is worthwhile to mention a relatively high sensitivity of the system to variations of certain parameters (internal damping) and to simulation time. For example, after a longer simulation time, more distinctive parametric resonance will be registered in the low frequency range (below 15 Hz), both in the numerical and experimental procedures. However, the experiments must not be too long either, because of a sharp increase in the oil and hose temperature which may change the properties of the system.

As the average flow velocity decreases (Figs. 6, 7), the probability of the parametric resonance occurrence is reduced, too. Actually, only the type 33\_1 resonance is revealed in the diagrams. Vibrations excited in the system have the frequency twice as large as the third natural frequency, which corresponds to the third mode of vibrations.

As the pulsation amplitude increases (Figs. 7, 8), the ranges of the parametric resonance tend to expand. The experimental diagrams reveal new resonance effects in the ranges predicted by the theoretical methods.

A thorough analysis of the plotted diagrams reveals certain discrepancies between the experimental and numerical data. For example, two resonance ranges are revealed on the experimental plots in the frequency range 14-28 Hz, whilst the plots of simulation results show four such ranges (resonance 22\_1, 23\_1, 33\_1, 34\_1 or 25\_1). Such close proximity of the principal and combination resonances causes that some of them will merge in the case of real objects. Further analogies are well apparent in Figs. 8a and 8b.

## 5. Conclusions

A thorough analysis of the numerical and experimental data leads us to the following conclusions:

- Liquid flow through a hose at near-critical velocities or higher gives rise to large-amplitude vibrations which, in most severe cases, may cause the hydraulic system to be damaged.
- At flow velocities below the critical value, parametric vibrations will be generated in a certain frequency range. In the low frequency range of the applied excitation, enveloping the principal and secondary resonances, the frequency of vibration is equal to half of the flow pulsation frequency or equal to it. In the higher frequency range, parametric resonance effects appear too, and are associated with subsequent natural frequencies of the system.

In this frequency range, the periodic vibrations will be excited, including sub-harmonic vibrations of various orders as well as quasi-periodic ones. Of particular interesting are the vibration modes registered in the combination resonance ranges.

- Major determinants of the extent of parametric resonance ranges and their distribution include flow velocity, pressure, internal damping, amplitude and frequency of flow pulsation.
- Comparison of the numerical and experimental results seems to confirm the adequacy of the adopted model of the system. The fundamental physical phenomena detectable by experimental methods were confirmed numerically. Besides, quantitative indicators of vibrations (rms velocity values) are well correlated too. Minor discrepancies revealed on the diagrams may be attributed on one hand to difficulties involved in assessment of the hose parameters and, on the other, to spatial features of vibration in certain ranges of the excitation frequency.
- Methods employed in the analysis, using the orthogonal polynomials as shape functions, allow a reliable qualitative assessment in a relatively short time. The stability testing method, based on Floquet's characteristic multipliers, proved most effective. They are determined by numerical integration of matrix equation (3.10) for one period only, making the numerical procedure much faster.

## References

1. CZERWIŃSKI A., ŁUCZKO J., 2012, Vibrations of steel pipes and flexible hoses induced by periodically variable fluid flow, *Mechanics and Control*, **31**, 2, 63-71
2. GINSBERG J.H., 1973, The dynamic stability of a pipe conveying a pulsatile flow, *International Journal of Engineering Science*, **11**, 1013-1024
3. GORMAN D.G., REESE J.M., ZHANG Y.L., 2000, Vibration of a flexible pipe conveying viscous pulsating fluid flow, *Journal of Sound and Vibration*, **230**, 2, 379-392
4. GREGORY R.W., PAIDOUSSIS M.P., 1966a, Unstable oscillation of tubular cantilevers conveying fluid: I. Theory, *Proceedings of the Royal Society (London)*, **A 293**, 512-527
5. GREGORY R.W., PAIDOUSSIS M.P., 1966b, Unstable oscillation of tubular cantilevers conveying fluid: II. Experiments, *Proceedings of the Royal Society (London)*, **A 293**, 528-542
6. HOLMES P.J., 1978, Pipes supported at both ends cannot flutter, *Journal of Applied Mechanics*, **45**, 619-622
7. KADOLI R., GANESAN N., 2004, Parametric resonance of a composite cylindrical shell containing pulsatile flow of hot fluid, *Composite Structures*, **65**, 391-404
8. LEE S. I., CHUNG J., 2002, New non-linear modelling for vibration analysis of a straight pipe conveying fluid, *Journal of Sound and Vibration*, **254**, 2, 313-325
9. ŁUCZKO J., CZERWIŃSKI A., 2012, Influence of boundary conditions on the natural frequencies and the stability regions of the hydraulic pipes (in Polish), *Czasopismo Techniczne*, **22**, 8-M, 71-90
10. MAILYBAYEV A.A., SEYRANIAN A.P., 2001, Parametric resonance in systems with small dissipation, *Journal of Applied Mathematics and Mechanics*, **65**, 5, 755-767
11. PAIDOUSSIS M.P., 1998, *Fluid-Structure Interactions: Slender Structures and Axial Flow*, vol. 1, Academic Press, London
12. PAIDOUSSIS M.P., 2003, *Fluid-Structure Interactions: Slender Structures and Axial Flow*, vol. 2, Elsevier Academic Press, London
13. PAIDOUSSIS M.P., ISSID N.T., 1974, Dynamic stability of pipes conveying fluid, *Journal of Sound and Vibration*, **33**, 267-294

14. PAIDOUSSIS M.P., ISSID N.T., 1976, Experiments on parametric resonance of pipes containing pulsatile flow, *Journal of Applied Mechanics*, **43**, 198-202
15. PAIDOUSSIS M.P., SUNDARARAJAN C., 1975, Parametric and combination resonances of a pipe conveying pulsating fluid, *Journal of Applied Mechanics*, **42**, 780-784
16. PANDA L.N., KAR R.C., 2008, Nonlinear dynamics of a pipe conveying pulsating fluid with combination, principal parametric and internal resonances, *Journal of Sound and Vibration*, **309**, 375-406
17. SEMLER C., LI G.X., PAIDOUSSIS M.P., 1994, The nonlinear equations of motion of pipes conveying fluid, *Journal of Sound and Vibration*, **169**, 577-599
18. UDAR R.S., DATTA P.K., 2007, Parametric combination resonance instability characteristics of laminated composite curved panels with circular cutout subjected to non-uniform loading with damping, *International Journal of Mechanical Sciences*, **49**, 3, 317-334
19. WANG L., 2009, A further study on the non-linear dynamics of simply supported pipes conveying pulsating fluid, *International Journal of Non-Linear Mechanics*, **44**, 115-121

*Manuscript received January 14, 2014; accepted for print February 20, 2014*